Materials Science and Engineering A 527 (2010) 7530–7537

Contents lists available at ScienceDirect

Materials Science and Engineering A

journal homepage: www.elsevier.com/locate/msea

Effects of thermal stress and imperfect interfacial bonding on the mechanical behavior of composites subjected to off-axis loading

Junjie Ye, Xuefeng Chen*, Zhi Zhai, Bing Li, Yanyang Zi, Zhengjia He

State Key Laboratory for Manufacturing Systems Engineering, Xi'an Jiaotong University, Xi'an, Shaanxi 710049, People's Republic of China

ARTICLE INFO

Article history:
Received 3 June 2010
Received in revised form 15 July 2010
Accepted 29 July 2010

Keywords:
Thermal residual stress
Interfacial debonding
Off-axis loading
Stress–strain response

ABSTRACT

Metal matrix composites exhibit inelastic response due to the viscoplasticity of matrix, and imperfect interfacial bonding will decrease the flow stress sharply. The present study develops the generalized model of cells (GMC) to predict mechanical behavior of unidirectional metal matrix composites with imperfect interfacial bonding, which is subjected to off-axis loading. The model incorporates viscoplastic model for the matrix and interfacial debonding model for the fiber/matrix interface. The effects of fiber volume fraction and thermal residual stress on stress–strain response of composites are also discussed. Results show that stress–strain response influenced by fiber cross-section shape becomes more evident with the increase of fiber off-axis angle. Similar stress–strain response can be found in the early stage of loading regardless of the thermal residual stress. However, the effect of thermal residual stress on the stress–strain behavior of composites with imperfect interfacial bonding is closely dependent on fiber off-axis angle in the plastic stage.

1. Introduction

Due to their low density, excellent mechanical strength, stiffness, creep resistance, as well as flexible design and manufacture according to service condition, composites have been new engineering materials widely used in aerospace, energy resources, transportation, machinery and biology. An unexpected failure may result in significant economic losses and safety problems. In order to minimize the accidents, many researchers have studied mechanical properties of composites [1,2,4,5]. However, they are restricted to study composites with perfect interfacial bonding. Many practical applications [6–8] show that structural difference between matrix and reinforced phase, as well as physical and chemical incompatibility lead to poor interfacial cohesive force. In other words, there is an imperfect interface between matrix and reinforced phase, which affects the mechanical properties of composites greatly.

Finite element method [9–12] and analytical micromechanical method [13–16,18] have been widely used to describe the effects of interface. Kang et al. [9] discussed the effect of interfacial bonding state between particulate and metal matrix on the ratchetting of SiC particulate reinforced 6061Al alloy composites by using a finite element code ABAQUS. The simulated results showed that composites with imperfect bonding are closer to the corresponding experiments than those obtained with assumption of perfect interface. Mondal et al. [10] modeled the interface in a metal matrix composites by using finite element method to study the deformation behavior of metal matrix composites as a function of interfacial characteristics. The interface is modeled as a thin layer of artificial material. The thickness and the modulus of the artificial material are varied as a means to vary the extent of coherency between the matrix and the particles. By implementing imperfect interfaces into finite element analysis, Nairn [11] proposed an approach to characterizing interfacial stiffness. Furthermore, some possible experiments for measuring the imperfect interfacial parameters needed for modeling were discussed. Caporale et al. [12] investigated the behavior of unidirectional fiber-reinforced composites with imperfect interfacial bonding through implementing an interfacial failure model by connecting the fibers and the matrix at the finite element nodes by normal and tangential brittle-elastic springs. Nie and Cemal [13] proposed a micromechanical model based on generalizations of Eshelby method to analyze effective elastic properties of particle filled acrylic composites with imperfect interfacial bonding. Based on a modified Needleman [14] type cohesive zone model, Lissenden [15] presented a three-dimensional fiber–matrix debonding model for weakly bonded composites. Model predictions for transverse tensile and axial shear responses of silicon carbide/titanium showed good agreement with the experiments. Through application of a displacement discontinuity between the fiber and matrix, Aboudi [16] incorporated flexible interface (FI) model [17] into the method of cells to investigate damage in composites with imperfect bonding. Later, constant

* Corresponding author. Tel.: +86 29 8266 7963; fax: +86 29 8266 3689.
E-mail address: chenxf@mail.xjtu.edu.cn (X. Chen).

0921-5093/$ – see front matter © 2010 Elsevier B.V. All rights reserved.
doi:10.1016/j.msea.2010.07.104

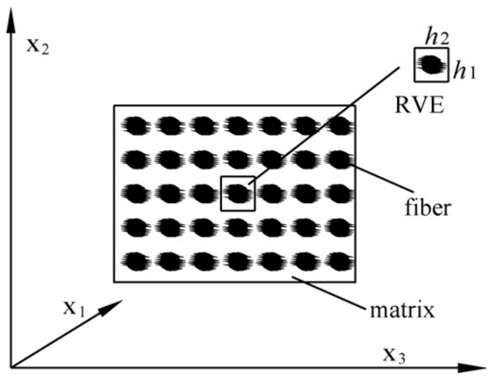

Fig. 1. Composite with periodic array.

compliant interface (CCI) [18] model, which was improved from FI model through adding a finite interfacial bond strength, was incorporated into GMC micromechanics model by Goldberg and Arnold [19] to investigate the tensile response of titanium matrix composite with imperfect interfacial bonding. However, both CCI and FI considered the interfacial debonding parameters to be constant. In other words, neither FI model nor CCI model can be used to describe progressive debonding of composites. To overcome this difficulty, Bednarcyk and Arnold [20] proposed a new interfacial debonding model named evolving compliant interface (ECI) model. The ECI model was implemented into GMC model to study the relationship between interface characteristic length and stress–strain response [21,22]. However, different fiber cross-section shapes of composites with imperfect interfacial bonding subjected to the influence of thermal residual stress arising from curing were not found in the studies above.

The present study investigates the influence of thermal residual stress on elasto-plastic response of composites with imperfect interface bonding. Furthermore, due to the complexity of loading and boundary condition, off-axis loading, which received relatively little attention, is also discussed.

The outline of this paper is organized as follows. A brief introduction of thermal residual stress calculation is given in Section 2. Section 3 presents the theory of incorporating interface debonding model into the GMC micromechanical model. In Section 4, the theory is used to investigate stress–strain response of composites subjected to different fiber off-axis angles. Meanwhile, both fiber cross-section shape and fiber volume fraction are also considered. Conclusions are given in Section 5.

2. Theoretical calculation of thermal residual stress

Generally speaking, the thermal expansion coefficient between fiber and matrix is always different. Once processing temperature changes, inconsistent thermal expansion or compression between fiber and matrix will lead to thermal stress. Many researches show that mechanical properties of composites depend deeply on thermal residual stress [23–25]. Therefore, the influence of thermal residual stress of composites should be calculated accurately.

The constitutive relationship of composites for each sub-cell can be written by:

$$\bar{\varepsilon}^{(\beta\gamma)} = S^{(\beta\gamma)}\bar{\sigma}^{(\beta\gamma)} + \bar{\varepsilon}^{p(\beta\gamma)} + \alpha^{(\beta\gamma)}\ \Delta T \quad (1)$$

In the composites, fibers are considered to be periodic distribution (see in Fig. 1). Based on the theory of generalized model of cells [26,27], the representative volume element (RVE) is usually divided into $N_\beta \times N_\gamma$ sub-cells as shown in Fig. 2. The relationship between sub-cell strain and overall strain can be expressed as:

$$\bar{\varepsilon}_{11}^{(\beta\gamma)} = \bar{\varepsilon}_{11} \quad (\beta = 1, \ldots, N_\beta; \quad \gamma = 1, \ldots, N_\gamma) \quad (2)$$

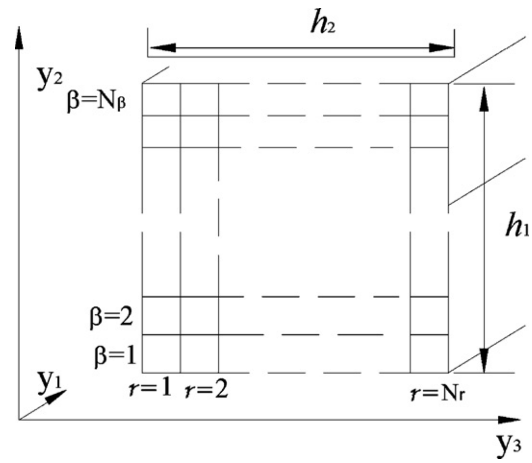

Fig. 2. Element division of RVE.

$$\sum_{\beta=1}^{N_\beta} h_\beta \bar{\varepsilon}_{22}^{(\beta\gamma)} = h\bar{\varepsilon}_{22} \quad (\gamma = 1, \ldots, N_\gamma) \quad (3)$$

$$\sum_{\gamma=1}^{N_\gamma} l_\gamma \bar{\varepsilon}_{33}^{(\beta\gamma)} = l\bar{\varepsilon}_{33} \quad (\beta = 1, \ldots, N_\beta) \quad (4)$$

$$\sum_{\beta=1}^{N_\beta} h_\beta \bar{\varepsilon}_{12}^{(\beta\gamma)} = h\bar{\varepsilon}_{12} \quad (\gamma = 1, \ldots, N_\gamma) \quad (5)$$

$$\sum_{\gamma=1}^{N_\gamma} l_\gamma \bar{\varepsilon}_{13}^{(\beta\gamma)} = l\bar{\varepsilon}_{13} \quad (\beta = 1, \ldots, N_\beta) \quad (6)$$

$$\sum_{\gamma=1}^{N_\gamma}\sum_{\beta=1}^{N_\beta} h_\beta l_\gamma \bar{\varepsilon}_{23}^{(\beta\gamma)} = hl\bar{\varepsilon}_{23} \quad (7)$$

where h_β and l_γ indicate the sub-cell sizes, respectively. h and l indicate the size of representative volume element, respectively. Superscript $(\beta\gamma)$ refers to the sub-cell.

For a fixed column of sub-cells $(1\gamma)\ldots(N_\beta\gamma)$ of normal stress $T_{22}^{(\gamma)}$ and fixed row of sub-cells $(\beta 1)\ldots(\beta N_\gamma)$ of normal stress $T_{33}^{(\beta)}$, stress continuity conditions can be expressed as:

$$\bar{\sigma}_{22}^{(1\gamma)} = \cdots = \bar{\sigma}_{22}^{(N_\beta\gamma)} = T_{22}^{(\gamma)} \quad (\gamma = 1, \ldots, N_\gamma) \quad (8)$$

$$\bar{\sigma}_{33}^{(\beta 1)} = \cdots = \bar{\sigma}_{22}^{(\beta N_\gamma)} = T_{33}^{(\beta)} \quad (\beta = 1, \ldots, N_\beta) \quad (9)$$

Substituting Eq. (1) into Eqs. (3) and (4), respectively, that is,

$$\sum h_\beta \left(S_{22}^{(\beta\gamma)} - \frac{S_{12}^{(\beta\gamma)^2}}{S_{11}^{(\beta\gamma)}} \right) T_{22}^{(\gamma)} + \sum h_\beta \left(S_{23}^{(\beta\gamma)} - \frac{S_{12}^{(\beta\gamma)} S_{13}^{(\beta\gamma)}}{S_{11}^{(\beta\gamma)^2}} \right) T_{33}^{(\beta)}$$
$$= h\bar{\varepsilon}_{22} - \sum h_\beta \frac{S_{12}^{(\beta\gamma)}}{S_{11}^{(\beta\gamma)}} \bar{\varepsilon}_{11} + \sum h_\beta \left(\frac{S_{12}^{(\beta\gamma)}}{S_{11}^{(\beta\gamma)}} \alpha_{11}^{(\beta\gamma)} - \alpha_{22}^{(\beta\gamma)} \right) \Delta T$$
$$+ \sum h_\beta \left(\frac{S_{12}^{(\beta\gamma)}}{S_{11}^{(\beta\gamma)}} \bar{\varepsilon}_{11}^{p(\beta\gamma)} - \bar{\varepsilon}_{22}^{p(\beta\gamma)} \right) \quad (10)$$